Adolescent Baseball Pitching Technique: A Detailed Three-Dimensional Biomechanical Analysis

CARL W. NISSEN[1,2], MELANY WESTWELL[1], SYLVIA ÕUNPUU[1], MAUSAM PATEL[1], JANET P. TATE[2], KRISTAN PIERZ[1,2], JOSEPH P. BURNS[3], and JAMES BICOS[4]

[1]Connecticut Children's Medical Center, Hartford, CT; [2]University of Connecticut, Farmington, CT; [3]Southern California Orthopaedic Institute, Van Nuys, CA; and [4]JRSI Sports Medicine, Indianapolis, IN

ABSTRACT

NISSEN, C. W., M. WESTWELL, S. ÕUNPUU, M. PATEL, J. P. TATE, K. PIERZ, J. P. BURNS, and J. BICOS. Adolescent Baseball Pitching Technique: A Detailed Three-Dimensional Biomechanical Analysis. *Med. Sci. Sports Exerc.*, Vol. 39, No. 8, pp. 1347–1357, 2007. **Purpose:** Document the biomechanics of the pitching motion to help provide insight about the etiology of common injuries seen in adolescent baseball pitchers. **Methods:** Kinematic and kinetic data for the upper and lower extremities, thorax, and pelvis were collected from 24 adolescent pitchers, using modern three-dimensional computerized motion-analysis techniques. **Results:** Original information regarding forearm and wrist motion was reported in this study and were consistent with expected motions for the fastball pitch. Average excursion of motion was: pronation/supination 63 ± 15°, wrist flexion/extension 44 ± 14°, and ulnar/radial deviation 12 ± 4°. Explosive forearm motion occurred between ball release (BR) and maximal glenohumeral internal rotation (GH-MIR) with a peak pronation velocity of 2051 ± 646°·s^{-1}. The majority of internal/external and abduction/adduction shoulder motion was attributed to the glenohumeral motion. Internal glenohumeral rotation range of motion was 125 ± 13° and mean peak internal glenohumeral rotation velocity was 3343 ± 453°·s^{-1}. Thorax and pelvic motion peak velocities and accelerations occurred before the peak elbow varus moment, which occurred at 59% of the pitch cycle (PC). The peak shoulder, elbow, and wrist velocities and accelerations occurred after the peak elbow varus moment. The pelvis squared to the plate at 51 ± 10% PC and the thorax at 59 ± 7% PC with maximal glenohumeral external rotation (GH-MER) at 65% PC and BR at 78 ± 3% PC. The data collected in this study were consistent with the literature, with the exception of joint velocities and moments, which were lower than those in one published study. **Conclusion:** We have established the kinematic and kinetic parameters of the adolescent baseball pitch. These measured parameters and the differences between adolescent pitchers and their adult counterparts can be used to examine and help determine the causes of the rapid increase in adolescent pitching injuries. **Key Words:** OVERHEAD SPORTS, KINETICS, KINEMATICS, MOTION ANALYSIS, JOINT MOMENTS, JOINT ANGLES

The recent incidence of adolescent pitcher arm injuries has increased at an alarming rate (1,7–9). The etiology of these injuries has not been clearly defined and is assumed to be multifactorial. Poor mechanics and overuse have been the most commonly cited causes of these problems. As a response, coaches have tried to teach "proper" mechanics at an early an age. Pitching coaches generally depend on experience, visual observation and in some cases video to provide the basis for technique modification or coaching tips. However, with the complex three-dimensional motions of the pitching arm and thorax, as well as the high speed of the pitching motion, many authors who have looked into this problem feel that more could be learned about the pitching motion using modern three-dimensional motion-analysis techniques.

The evaluation of the three-dimensional pitching mechanics in adolescent pitchers using modern motion-analysis techniques has been limited. Consequently little understanding of the kinematics and kinetics of "normal" adolescent pitching technique, not to mention the "abnormal" mechanics that may lead to injuries, exists. Fleisig et al. (4) examined 23 youth pitchers (ages 10–15), using a variety of kinematic, kinetic, and temporal parameters to examine the fastball pitch. They found that these pitchers generally pitched in a similar manner to adult pitchers, with peak values of certain kinematic and kinetic parameters being lower in the adolescent pitchers (4). Sabick et al. (12), evaluated 14 pitchers who were 12 yr old and analyzed a variety of kinematic and kinetic parameters to examine the relationships between elbow valgus torque and other kinematic parameters. The above papers have contributed to our understanding of the adolescent pitching motion from a biomechanical point of view, however, wrist motion was

Address for correspondence: Carl W. Nissen, M.D., Elite Sports Medicine, 100 Simsbury Rd, Suite 208, Avon, CT 06001; E-mail: cnissen@ccmckids.org.
Submitted for publication September 2006.
Accepted for publication March 2007.

0195-9131/07/3908-1347/0
MEDICINE & SCIENCE IN SPORTS & EXERCISE®

DOI: 10.1249/mss.0b013e318064c88e

not included and the shoulder model was limited to assessment of the humerus versus the torso. Also, these papers did not provide plotted kinematics of the pelvis, thorax, and kinematics and kinetics of the upper extremities, which are the best way to document and understand movement during a period of time such as the pitch cycle.

The pitching model developed in our lab for this study includes a three-dimensional wrist component, which allows for measurement of wrist flexion/extension and radial/ulnar deviation as well as forearm supination/pronation. The kinematics and kinetics of the wrist component have not been previously reported for the baseball pitching motion. The model also includes a scapular segment and a glenohumeral joint. A spherical centering technique is used to determine the location of the glenohumeral joint center, which is embedded in the scapula segment (13). These adaptations have resulted in a more consistent humeral segment length. Pilot data collected during the development of this model showed that the spherical centering technique helped reduce the error in humerus length compared with the typical shoulder joint method, which embeds the glenohumeral joint center at an arbitrary location within the thorax segment (3,11,12). The humerus segment length was noted to change by 13% during the pitching motion when applying typical shoulder-joint methods (4,11), whereas the spherical centering offset embedded in a scapula segment helped reduce the humeral length change to 4%.

The most common theories as to the cause of this epidemic of injuries in adolescent pitchers—poor mechanics and excessive pitching—have not been adequately evaluated at this point, because basic understanding of the adolescent pitching biomechanics does not exist. Before these theories can be supported or refuted, a detailed documentation and understanding of the three-dimensional kinematics and kinetics of the pitching motion is needed in adolescent pitchers. The purpose of this study was to describe the kinematics and kinetics of the pitching motion in adolescent baseball pitchers.

MATERIALS AND METHODS

Subjects. Twenty-four subjects under the age of 14 were recruited from local youth baseball programs. Each pitcher had at least 2 yr of pitching experience in organized baseball and no history of arm surgery or current arm pain. Only right-handed pitchers were used in this study.

The institutional review board at the Connecticut Children's Medical Center and the University of Connecticut Health Center approved the project. All subjects signed assent forms, and informed consent was obtained from their parents prior to involvement in the study.

Data collection. A medical and pitching history was obtained. A physical exam was performed and anthropomorphic measurements including height, weight, leg lengths, arm lengths, and joint diameters were obtained from each subject.

The subjects wore athletic shorts and sneakers, and a total of 38 reflective markers were attached to the specific body landmarks to form 16 body segments (Fig. 1, Appendix A). The marker placements enabled estimation of joint centers and three-dimensional body-segment locations, allowing for measurements of the kinematics throughout the pitching motion (segment motion and joint angles). Two markers were placed along the baseball diameter to track the ball motion.

Each subject was then given time to stretch and throw until adequately warmed up. Pitchers were instructed to throw only fastballs. Subjects pitched from a flat surface (no mound) in the center of the laboratory down a 45-foot length into a net that had a designated strike zone. After the

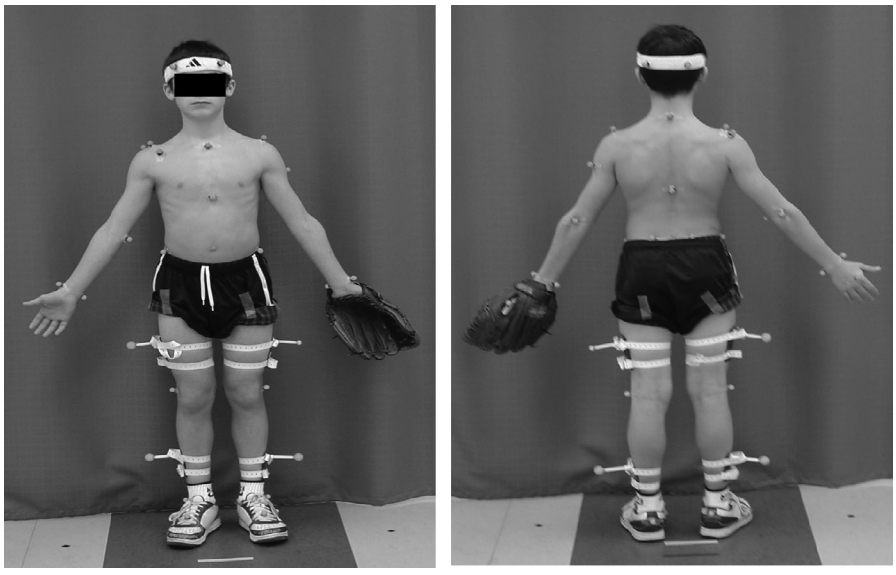

FIGURE 1—Marker placement.

subject felt adequately warmed up, motion data were collected from a total of 10 fastball pitches.

A 512 Vicon Motion Systems (Vicon Motion Systems, Lake Forest, CA) was used for data collection. This system uses 12 synchronized cameras placed circumferentially around the lab and allows for 250-Hz data capture.

Data analysis. Initial data processing was performed in Workstation (Vicon Motion Systems, Lake Forest, CA) including marker reconstruction, creation of marker trajectories, and generation of kinematics using the model described above (see also Appendix A). The joint angles were calculated using Euler equations of motion. The rotational sequences were chosen for each joint so that the calculated angles best represented clinically relevant motions. Rotation sequence used for all joints was sagittal, coronal, and transverse (*y*, *x*, *z*) except for glenohumeral, which was coronal, sagittal, transverse (*x*, *y*, *z*).

A fourth-order, zero-lag Butterworth digital filter was used to smooth the raw data with a cutoff frequency of 15 Hz. Qualitative evaluations of displacement, velocity, and acceleration data were performed to find the optimal cutoff frequency, which was effective at rejecting the noise and passing data. Joint kinetics were computed using custom Matlab codes, using standard inverse dynamics techniques.

The pitching motion was divided into several phases as previously defined (3). Data analysis was limited to the arm-cocking phase (lead foot contact (FC) to maximum glenohumeral external rotation (GH-MER)), arm-acceleration phase (GH-MER to ball-release (BR)), and arm-deceleration phase (BR to maximum glenohumeral internal rotation (GH-MIR)). Lead FC was the time when any part of the foot (heel or the toe) contacted the ground, as pitchers were found to vary. Ground contact was defined by a velocity of the heel or toe marker of the lead foot that was less than 1.5 $m \cdot s^{-1}$. BR was defined as the instant when the distance between any of the markers on the baseball and the marker on the hand increased by greater than 2 cm. The pitching cycle from FC to GH-MIR was time normalized.

Several kinematic and temporal parameters were selected for analysis. These parameters were selected as potentially significant from throwing studies in the existing literature (4,10) and instructional videos and discussions with USA Baseball Hall of Fame Coach Bill Thurston, an internationally renowned authority on pitching mechanics.

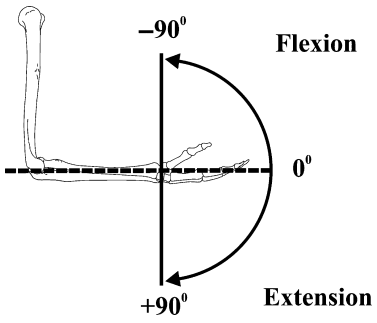

FIGURE 2—Wrist flexion and extension.

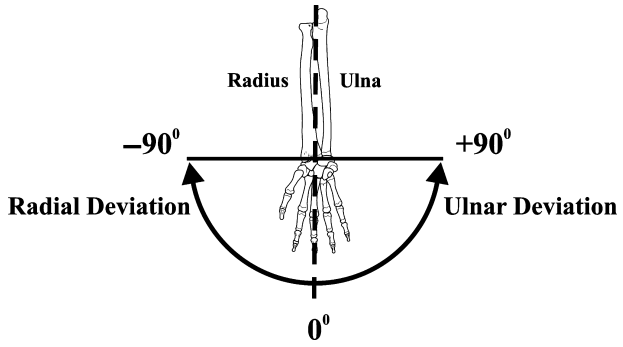

FIGURE 3—Wrist radial and ulnar deviation.

The following three-dimensional joint and segment Euler angles (flexion/extension, abduction/adduction or valgus/varus, and internal/external rotation) were analyzed in this study, with the following angle sequence:

a. Wrist angle = joint angle between the hand and forearm (Figs. 2 and 3)
b. Forearm motion = pronation/supination of the radius and ulna (Fig. 4)
c. Elbow angle = joint angle between the humerus and forearm (Fig. 5)
d. Glenohumeral angle = joint angle between the scapula and humerus (Figs. 6–8)
e. Thorax angle = angle formed between the thorax and global coordinate system
f. Pelvic angle = angle formed between the pelvis and global coordinate system
g. Spine angle = joint angle formed between the thorax and pelvis (thorax angle minus pelvis angle)

Figures 2–8 demonstrate graphically the definitions of upper-extremity joint angles used in our study. Transverse plane rotation of the thorax and pelvis were measured with respect to the home plate. The pelvis and thorax were in 0° of transverse rotation when they were squared to the home plate. For example, when the right and left anterior superior iliac spines were parallel to the home plate, the pelvic rotation equaled 0°. The ball velocity was measured at BR.

Statistical analysis. Three trials in which all 38 markers were visible for the entire pitching cycle were

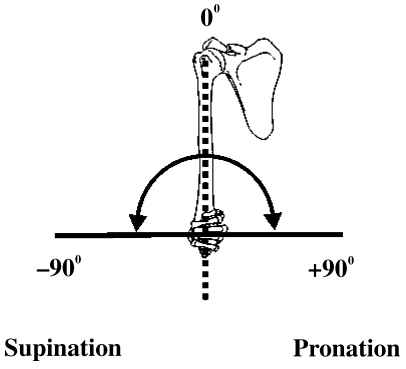

FIGURE 4—Forearm pronation and supination.

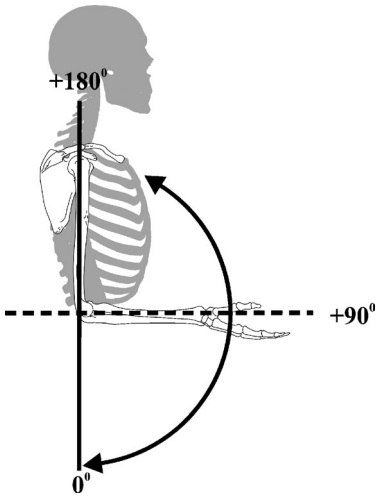

FIGURE 5—Elbow flexion and extension.

analyzed for each subject. The mean of these three trials was used to compute the group mean and standard deviation for each parameter. The mean kinematic and kinetic plots for the pitch cycle for selected parameters were also computed for each subject and then used to plot the mean group kinematic and kinetic plots. Comparisons were made with the previously published literature for adult pitchers and the data available for adolescent pitchers.

RESULTS

The mean age for the 24 boys included in this study was 12 yr 3 months (range 8 yr 1 month to 13 yr 6 months). The average weight was 48 ± 14 kg (range 28.5–84), and the average height was 154 ± 12 cm (range 133–177). Body mass index average was 20.1 $kg \cdot m^{-2}$ (range 16.1–26.8 $kg \cdot m^{-2}$).

Kinematics

Wrist. The largest motion at the wrist was seen in the sagittal plane with a mean ROM of 44 ± 14° (Fig. 9 and Table 1). The wrist maintained consistent extension (mean of 30 ± 18°) from FC through GH-MER, at which time rapid wrist flexion occurred until midway between BR and GH-MIR. A recoil of wrist extension continued through to GH-MIR. The mean peak wrist-flexion velocity was 1359 ± 453° $\cdot s^{-1}$. There was a limited amount of coronal-plane wrist motion noted (mean range of motion was 12 ± 4°) with more radial deviation (8 ± 6° at FC) followed by gradual ulnar deviation to near neutral at BR.

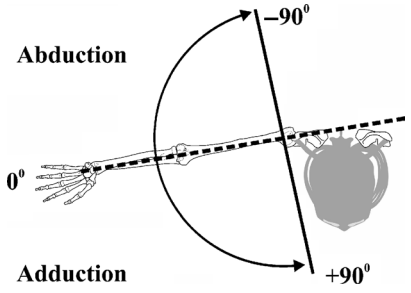

FIGURE 6—Glenohumeral horizontal abduction/adduction.

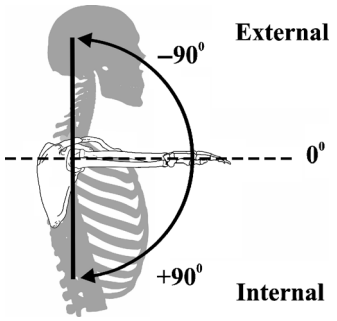

FIGURE 7—Glenohumeral internal and external rotation. Glenohumeral rotation is defined as the angle between the scapula and the humerus. The *solid vertical line* represents the medial/lateral axis of the humerus and its rotation with respect to the scapula (as defined by the *arc*) represents glenohumeral rotation.

Forearm. Our pitchers demonstrated a mean forearm pronation at FC of 14 ± 19° with decreased pronation (supination) at GH-MER to a mean of −1 ± 13° (Fig. 9 and Table 1). From GH-MER through BR, minimal pronation motion occurred and was followed by more rapid pronation from BR (mean of 7 ± 13) to GH-MIR (mean of 50 ± 15). Throughout the pitch cycle (PC), minimal supination occurred, with some pitchers never achieving any supination. The mean pronation/supination range of motion for the forearm was 63 ± 15°, with the majority occurring after BR in the pronation direction. The peak pronation velocity was 2051 ± 646° $\cdot s^{-1}$ and occurred well after BR at 88 ± 4% PC. There was minimal supination motion and velocity.

Elbow. The primary movement of the elbow during the PC was rapid extension, beginning before GH-MER to just after BR (Fig. 9 and Table 2). The overall elbow flexion/extension range of motion was 79 ± 14°, with a mean elbow flexion at foot contact of 85 ± 26°. The peak elbow-extension velocity was 1782 ± 245° $\cdot s^{-1}$ and occurred at 75 ± 4% PC, which was just before BR.

Glenohumeral. The largest motion for the glenohumeral joint was seen in the internal/external rotation

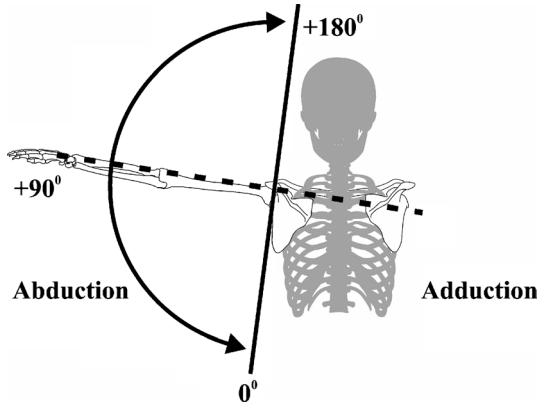

FIGURE 8—Glenohumeral vertical abduction/adduction.

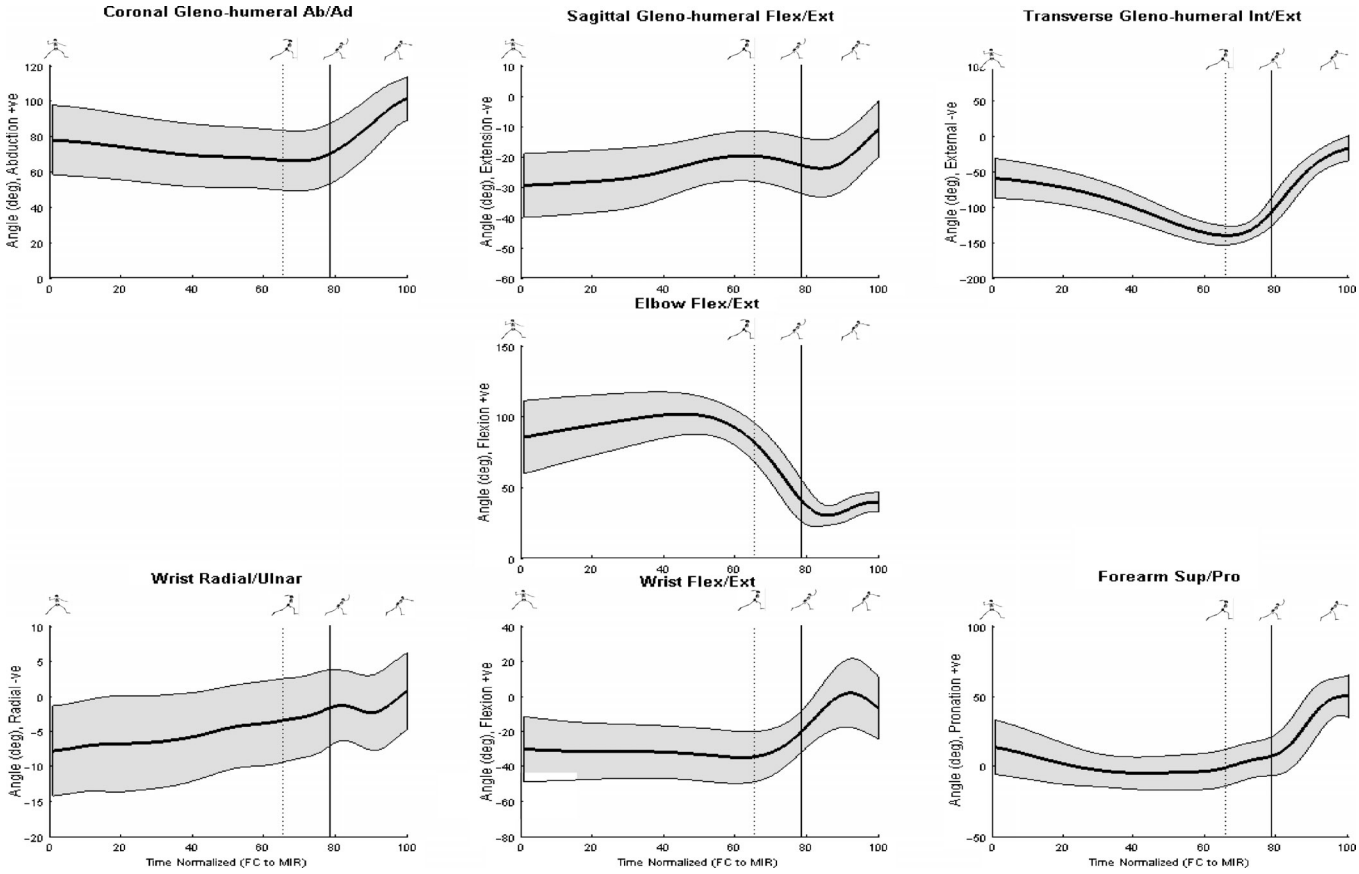

FIGURE 9—Upper-extremity kinematics. Mean kinematic plots of 24 subjects for the glenohumeral, elbow, and wrist joints for abduction/adduction or radial/ulnar (*first column*), flexion/extension (*second column*), and internal/external or pronation/supination (*third column*) motions. All data was normalized to the pitch cycle from foot contact (0%) to maximum internal glenohumeral rotation (100%). The *vertical lines* indicate the mean maximum glenohumeral external rotation and ball release of the 24 subjects.

plane, with a mean range of motion of 125 ± 13° (Fig. 9 and Table 3). The mean GH external rotation at foot contact was −60 ± 28°. From FC to GH-MER, there is progressive external rotation, which is followed by rapid internal rotation through GH-MIR. The mean maximum internal rotation velocity was 3343 ± 453°·s^{-1}. Velocities in the other planes of GH motion were substantially lower. The GH joint showed similar abduction from FC (mean of 78 ± 20°) through BR (mean of 70 ± 17°). Increasing GH abduction was noted from BR through GH-MIR. In the horizontal abduction/adduction plane, (equivalent to sagittal flexion/extension plane) the GH joint was in horizontal abduction (extension) at FC (mean of −30 ± 10°), followed by progressive horizontal adduction (flexion) throughout the majority of the PC, to −11 ± 9 at GH-MIR.

Pelvis/Thorax. In the transverse plane, the thorax and pelvis showed progressive internal rotation from FC through BR (Fig. 10 and Tables 4 and 5). Squaring of the pelvis to the plate occurred, on average, at 51 ± 10% PC, and squaring of the thorax occurred at 59 ± 7% PC, both before GH-MER (mean of 65 ± 4% PC) and BR (mean of 78 ± 3% PC) (Table 6). In the sagittal plane, the pelvis showed progressive anterior tilting from FC through BR, with a mean range of motion of 31 ± 7°. The thorax followed a similar pattern, with progressive anterior tilting that began and ended later in the pitch cycle, with an increased mean range of motion of 58 ± 12°. In the coronal plane, the pelvis showed the least range of motion. The thorax, however, showed a mean range of motion of 31 ± 12°, with a progressive lateral lean away from the pitch arm side from FC through GH-MER. The thorax remained in a similar degree of lateral lean from GH-MER through GH-MIR.

Kinetics

Wrist. Moments at the wrist were relatively much lower than those for the elbow (Fig. 11 and Tables 1 and 2). The peak wrist moment was noted in the sagittal plane, with a mean extension moment of 2.4 ± 1.9 N·m just after BR.

Elbow. The greatest loads as expressed by net internal joint moments (mean of 27 ± 12 N·m) were noted in the coronal plane just before GH-MER at 59 ± 4% PC (Fig. 11 and Table 2). Peak elbow flexor and extensor moments were similar with respect to timing, but much less than the coronal-plane elbow moments.

Glenohumeral. The mean peak internal rotational torque at the glenohumeral joint was 27 ± 12 N·m (Fig. 11 and Table 2). The timing of this peak was 60 ± 4% PC.

TABLE 1. Comparison of wrist and forearm kinematics and kinetics (ulnar/radial, flex/extension, and pronation/supination motion) for specific points in the pitching cycle.

	Wrist Coronal-Plane Ulnar (+ve), Radial (−ve) Deviation	Wrist Sagittal-Plane Flexion (+ve), Extension (−ve)	Elbow Tranverse-Plane Pronation (+ve), Supination (−ve)
Angles			
Angle at FC (°)	−8 ± 6	−30 ± 18	14 ± 19
Angle at MER (°)	−4 ± 6	−35 ± 14	−1 ± 13
Angle at BR (°)	−1 ± 5	−21 ± 12	7 ± 13
Angle at MIR (°)	1 ± 5	−7 ± 17	50 ± 15
ROM (°)	12 ± 4	44 ± 14	63 ± 15
Joint velocities			
Maximal ulnar, flexion, pronation velocity (°·s^{-1})	335 ± 137	1359 ± 453	2051 ± 646
Maximal ulnar, flexion, pronation velocity (% PC)	87 ± 20	83 ± 5	88 ± 4
Joint kinetics			
Maximal radial, extension, pronation moment (N·m)	−2.2 ± 1.5	−2.4 ± 1.9	1.5 ± 0.7
Maximal radial, extension, pronation moment (% PC)	85 ± 24	82 ± 3	77 ± 9

FC, foot contact; MER, maximum external rotation of the glenohumeral joint; BR, ball release; MIR, maximal internal rotation of the glenohumeral joint; ROM, range of motion; max, maximum; PC, pitch cycle.

A comparison between results for the current study and those found in both Fleisig et al. (4), and Sabick et al. (12), for selected kinematic and kinetic parameters for the shoulder and elbow, shows some similarities and some differences in outcomes in Table 6.

DISCUSSION

The increased incidence of injuries in adolescent pitchers has caused significant concern and discussion about its etiology. Only a single report on the basics of the adolescent pitching motion exists which stated that the kinematic parameters for these pitchers when compared with their older counterparts were directly related to the slower velocities at which they pitched (4). Although epidemiological studies have shown that there seems to be a correlation between the number of pitches thrown and the injury rate, the explanation for the increasing rate of injuries in these younger athletes may have additional causes, which have not been elucidated. A more detailed understanding of this complex motion is necessary so that mechanisms of injury possibly related to motions and loads can be better understood and, therefore, treated. Therefore, the purpose of this study was to document the pitching motion in adolescent pitchers.

TABLE 2. Comparative table of shoulder and elbow pitching data for adolescent pitchers collected from Sabick et al. (12) (first column), Fleisig et al. (4) (second column), and the data collected for this study (third column).

	Sabick et al. ± SD	Fleisig et al. ± SD	Mean ± SD
Shoulder			
Maximum external rotation (°)	166 ± 9	177 ± 12	−168 ± 10
Maximum internal rotation velocity (°·s^{-1})		6900 ± 1050	3778 ± 487
Vertical abduction at MER (°)	92 ± 8		87 ± 10
Horizontal abduction at MER (°)	4 ± 12		4 ± 9
Maximum internal rotation torque GH (N·m)		30 ± 7	27 ± 12
Elbow			
Elbow flexion at FC (°)	79 ± 29	74 ± 17	85 ± 26
Elbow flexion at MER (°)	57 ± 22	95 ± 12	81 ± 11
Elbow flexion at BR (°)	25 ± 14	24 ± 7	39 ± 10
Maximum elbow extension velocity (°·s^{-1})		2230 ± 300	1782 ± 245
Maximum varus torque (N·m)	18 ± 4	28 ± 7	27 ± 12
Ball velocity (m·s^{-1})	21.6	28 ± 1	23 ± 3

FC, foot contact; MER, maximum external rotation; BR, ball release; GH, glenohumeral.

TABLE 3. Glenohumeral joint kinematics (vertical abduction/adduction, horizontal abduction/adduction, and internal/external motion) for specific points in the pitching cycle.

	Coronal-Plane Abduction (+ve)/ Adduction (−ve)	Sagittal-Plane Flexion (+ve)/ Extension (−ve)	Tranverse-Plane Internal (+ve)/ External (−ve)
Joint angle			
Angle at FC (°)	78 ± 20	−30 ± 10	−60 ± 28
Angle at MER (°)	66 ± 17	−20 ± 9	−141 ± 14
Angle at BR (°)	70 ± 17	−23 ± 9	−109 ± 10
Angle at MIR (°)	101 ± 12	−11 ± 9	−17 ± 18
ROM (°)	40 ± 12	21 ± 10	125 ± 13
Joint velocity			
Maximum vertical abduction, horizontal abduction, internal angular velocity (°·s^{-1})	1035 ± 323	661 ± 262	3343 ± 453
Maximum vertical abduction, horizontal abduction, internal angular velocity (% PC)	89 ± 15	94 ± 11	82 ± 4

FC, foot contact; MER, maximum external rotation of the glenohumeral joint; BR, ball release; MIR, maximal internal rotation of the glenohumeral joint; ROM, range of motion; max, maximum; PC, pitch cycle.

The results of this study demonstrate that adolescent children incorporate complex movements of the pitching wrist, elbow, and shoulder as well as pelvis and thorax to achieve a fastball pitch. Examining the joint range of motions, angular velocities, and joint moments showed values that were substantially more than that experienced by the lower extremities for activities such as walking. One of the contributions of this study was the documentation of three-dimensional wrist motion, which has not been previously documented for the adolescent pitcher. Wrist motion was found to be consistent with motions expected for the fastball pitch, with the largest range of motion and greatest velocity in the flexion/extension plane during wrist flexion. Minimal ulnar and radial deviation was found. However, forearm pronation/supination motion showed substantial pronation motion and velocity that were greater than that seen in wrist flexion/extension motion. The mean pronation velocity was also greater than the elbow-extension velocity, which showed rapid extension from before GH-MER to after BR. Forearm pronation began at BR. The implication of substantial forearm pronation velocities with respect to injury etiology at the elbow are

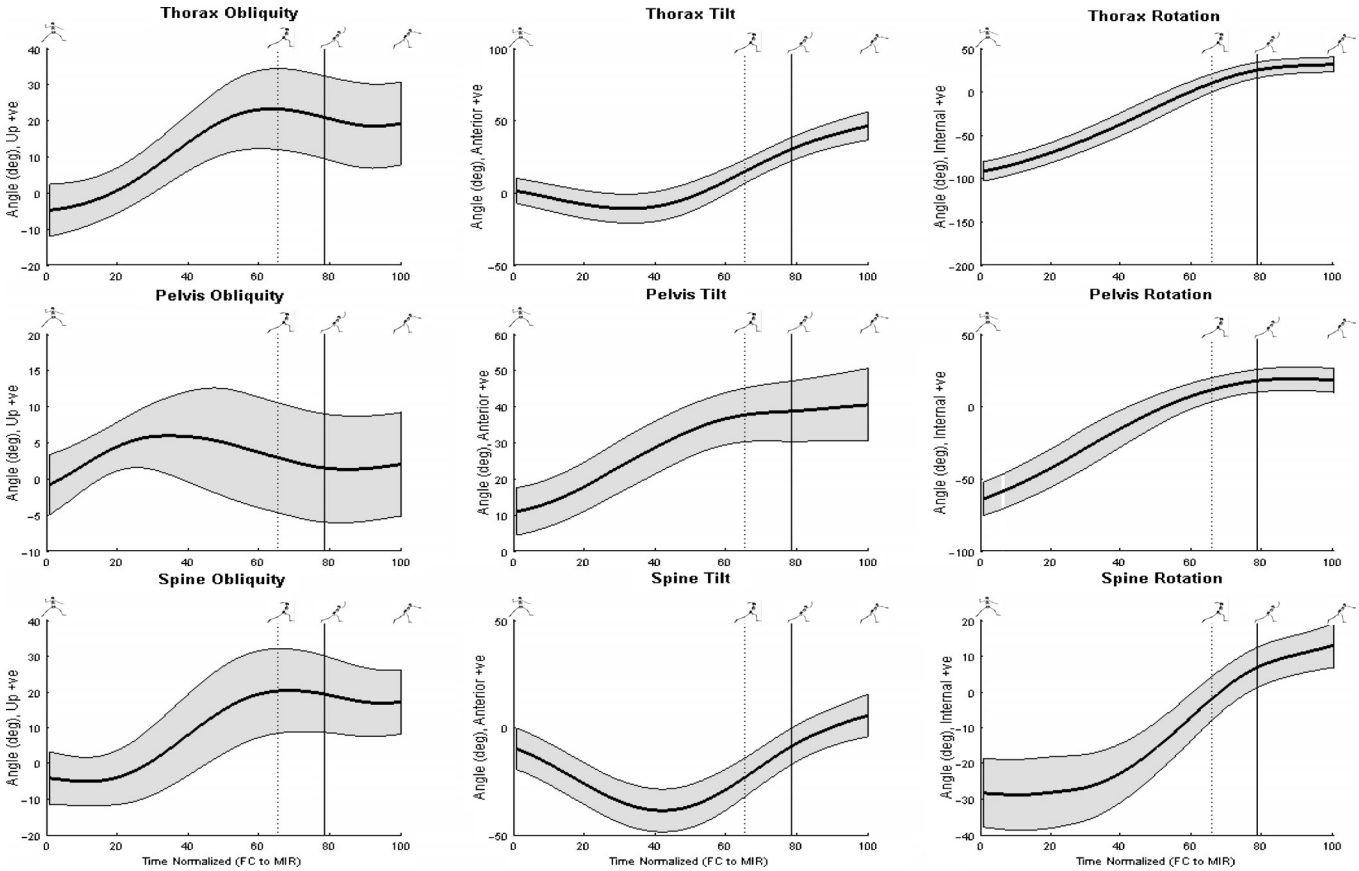

FIGURE 10—Thorax, spine, and pelvis kinematics. Mean kinematic plots of 24 subjects for the thorax, pelvis, and spine for the coronal (*first column*), sagittal (*second column*), and transverse (*third column*) planes. All data were normalized to the pitch cycle from foot contact (0%) to maximum internal glenohumeral rotation (100%). The *vertical lines* indicate the mean maximum glenohumeral external rotation and ball release of the 24 subjects.

not well understood and warrant further investigation with respect to the soft-tissue structures that may be impacted.

Ultimately, a better understanding of shoulder injury during pitching will come through a more comprehensive model of the shoulder complex. In this study, we studied the differences between shoulder motion and glenohumeral motion. The shoulder joint was defined in this study as the relative motion between the humerus and thorax, which is commonly reported in the pitching literature to date. The glenohumeral joint was defined in this study as the relative motion between the humerus and scapular segments, which has not been reported in the pitching literature to date. The glenohumeral joint showed the largest range of motion in the internal/external rotation plane with internal rotation from GH-MER to GH-MIR. Related to this was also the largest peak angular velocity in the direction of internal rotation

TABLE 4. Comparison of the thorax kinematics for the coronal, sagittal, and transverse plane for specific points in the pitching cycle.

	Coronal-Plane Up (+ve), Down (−ve)	Sagittal-Plane Anterior (+ve), Posterior (−ve)	Tranverse-Plane Internal (+ve), External (−ve)
Joint angles			
Angle at FC (°)	−5 ± 7	1 ± 9	−92 ± 11
Angle at MER (°)	23 ± 11	16 ± 8	10 ± 12
Angle at BR (°)	21 ± 11	30 ± 8	25 ± 9
ROM (°)	31 ± 12	58 ± 12	123 ± 12
Joint velocities			
Maximum up, anterior, internal velocity ($°\cdot s^{-1}$)	355 ± 137	603 ± 149	938 ± 109
Maximum up, anterior, internal velocity (% PC)	35 ± 6	65 ± 9	48 ± 9

FC, foot contact; MER, maximum external rotation of the glenohumeral joint; BR, ball release; MIR, maximal internal rotation of the glenohumeral joint; ROM, range of motion; max, maximum; PC, pitch cycle.

TABLE 5. Comparison of the pelvis kinematics for the coronal, sagittal, and transverse plane for specific points in the pitching cycle.

	Coronal-Plane Up (+ve), Down (−ve)	Sagittal-Plane Anterior (+ve), Posterior (−ve)	Tranverse-Plane Internal (+ve), External (−ve)
Joint angles			
Angle at FC (°)	−1 ± 4	11 ± 7	−64 ± 12
Angle at MER (°)	3 ± 8	38 ± 8	11 ± 9
Angle at BR (°)	1 ± 8	39 ± 8	18 ± 8
ROM (°)	12 ± 4	31 ± 7	84 ± 11
Joint velocities			
Maximum up, anterior, internal velocity ($°\cdot s^{-1}$)	170 ± 62	267 ± 73	678 ± 90
Maximum up, anterior, internal velocity (% PC)	11 ± 15	30 ± 3	31 ± 10

FC, foot contact; MER, maximum external rotation of the glenohumeral joint; BR, ball release; MIR, maximal internal rotation of the glenohumeral joint; ROM, range of motion; max, maximum; PC, pitch cycle.

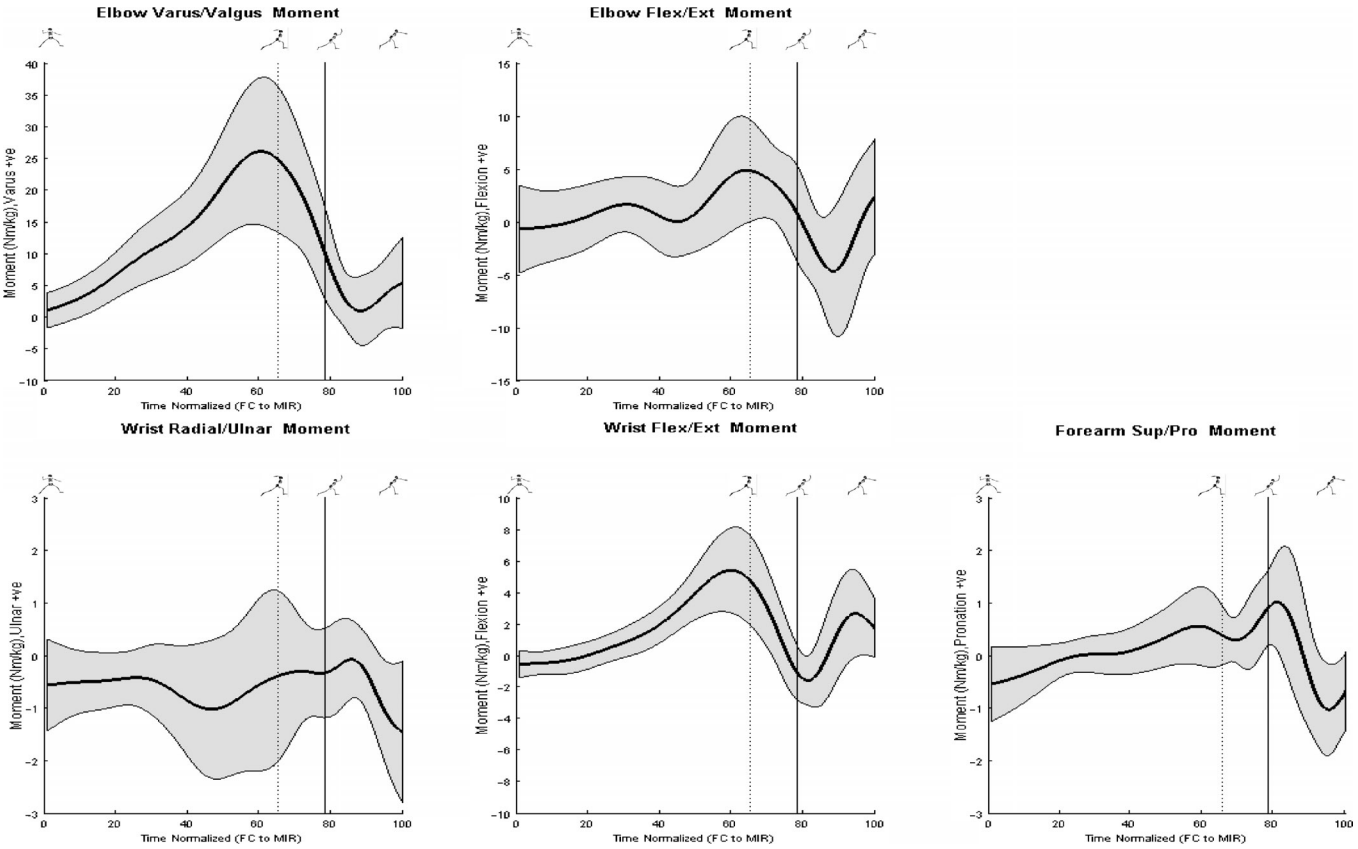

FIGURE 11—Upper-extremity kinetics. Mean kinetic plots of 24 subjects for the elbow and wrist joints for radial/ulnar or varus/valgus (*first column*), flexion/extension (*second column*), and supination/pronation (*third column*) motions. All data were normalized to the pitch cycle from foot contact (0%) to maximum internal glenohumeral rotation (100%). The *vertical lines* indicate the mean maximum glenohumeral external rotation and ball release of the 24 subjects.

occurring just after BR. The range of motion and velocities in the horizontal and vertical abduction/adduction plane were much less. Most of the shoulder rotation came from the glenohumeral joint; the overall maximum external rotation of the glenohumeral joint (141 ± 14°) was similar to the shoulder maximum external rotation (168 ± 10°). The remainder (about 27°) of the shoulder external rotation most likely came from the relative motion between the scapula and thorax. Similarly, the majority of the shoulder vertical abduction motion came from the glenohumeral joint. In the horizontal abduction/adduction plane, there was substantial contribution of the scapula–thoracic motion to the shoulder horizontal abduction/adduction motion. The varying contributions and timing of the scapular thoracic movement in the different planes of motion is not fully understood, but they may have injury implications.

Understanding of complex motions goes beyond ranges and peaks and must include timing information. The relative timing of pelvis and thorax squaring to the plate in relationship to GH-MER and BR allowed us to assess the impact of coiling on ball velocity. This information was provided using transverse plane kinematics of the pelvis and thorax. The relative difference in rotation between the pelvis and thorax at foot contact was 28° with more external rotation of the thorax in relationship to the pelvis. This difference in rotation allows for "coiling" from foot contact through GH-MER and serves to build potential energy for subsequent transfer into the arm and then into the baseball. For these pitchers, the pelvis was squared to the plate at 51% PC, followed by the thorax at 59% PC. We found that just after GH-MER, the relative difference had been equalized (pelvis and thorax were aligned rotationally) at 68% PC with the coiling of the thorax completed and transfer of the stored energy to the arm. After equalization at approximately MER, through BR the thorax and pelvis continued to rotate with slightly increased rotation of the thorax relative to the pelvis at BR, both of which were no longer square to the plate but overrotated by 18 ± 8° for the pelvis and 25 ± 9° for the thorax (Fig. 12). Of

TABLE 6. Timing as represented by percentage of the pitch cycle (PC) of the thorax, pelvic, and spine at the point in transverse plane motion of squaring to home plate or 0° of rotation.

	Mean ± SD
Thorax squaring (% PC)	59 ± 7
Pelvis squaring (% PC)	51 ± 10
Spine straightening (% PC)	68 ± 9
MER (% PC)	65 ± 4
BR (% PC)	78 ± 3

MER, maximum external rotation of the glenohumeral joint; BR, ball release.

interest, the peak coronal-plane elbow moment occurred simultaneously with the squaring of the thorax to the plate. The implications of this rotational sequence as well as thorax and pelvis motions in the coronal and sagittal planes need to be studied, to determine the impact of this complex interaction on elbow loads and other joints prone to injury.

The relative timing of all the segments and joints related to the pitching motion is the next step and will lead to a greater understanding of the complex nature of the pitching motion and insight into potential injury mechanisms. All the peak velocities and accelerations of the thorax, pelvis, and spine occurred before peak elbow varus moment, which occurs at 59% PC. The mean peak shoulder internal-rotation, wrist-flexion, and forearm-pronation velocities occurred after BR at 82, 83, and 88% PC, respectively. The associated peak accelerations also occurred after peak elbow varus moment. This would suggest that the thorax/pelvis provide the largest input to the coronal-plane elbow moment. An understanding of the complex relationship between the magnitudes and relative timing of all these motions, velocities, and accelerations and their impacts on joint moments may lead to a better understanding of injury mechanisms related to motion and better strategies for reducing soft-tissue and structural loads.

Joint moments were also computed for the wrist, elbow, and glenohumeral joints. The peak elbow varus and peak glenohumeral internal moments were significantly larger than wrist ulnar/radial, elbow flexion/extension, and forearm pronation/supination moments. The large elbow varus moment is generally thought to be the potential cause of "Little League elbow" injuries because it implicates increased loads on the elbow joint. The peak elbow varus moment and glenohumeral internal moment profiles were very similar in terms of magnitude and timing, with peak values at 59% PC, which occurs before GH-MER. This would implicate addressing activities that occur before GH-MER, such as pelvic and thorax squaring to the plate, to reduce loads on the elbow and potential elbow injuries related to large coronal-plane moments. Initial assessments suggest that trunk and pelvic transverse-plane rotations do correlate with elbow varus moments.

The data for this study were also compared with data collected in other studies of adolescent and adult pitchers. In general, findings were similar, with differences reflecting both differences in skeletal models used and, possibly, some differences in pitching skill between study groups. Elbow kinematic data were similar with respect to pattern of motion; however, the data in the current study showed more flexion at the point of BR than that reported in the literature for other youth (4). This will partly explain the associated reduction in the mean angular elbow-extension velocity for the current study group compared with that reported in the literature for both youths and adults (2,4,6). The net effect of these differences was a lower ball velocity (23 ± 3 m·s^{-1}) noted in this study compared with those in the Fleisig et al. study (28 ± 1 m·s^{-1}). It is possible that the pitchers in this study may have been less experienced pitchers. The mean peak elbow angular-extension velocity occurred just before BR, for our adolescent pitchers, which was similar to that reported for adults (5,6).

The mean peak elbow varus moment (27 ± 12 N·m) for the youth pitchers in this study was higher than that previously published by Sabick et al. (18 ± 4 N·m) (12) but similar to that reported by Fleisig et al. (28 ± 7 N·m) (4). The similar

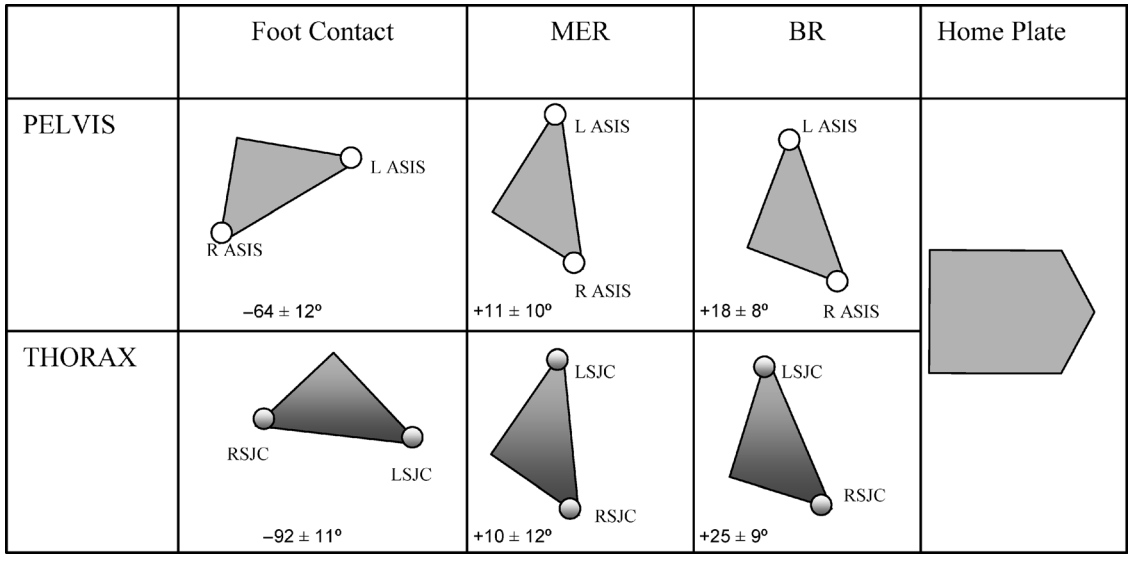

FIGURE 12—Diagrammatic representation of transverse-plane relationship between pelvis and thorax body segments. The figure illustrates the mean relative positions of the pelvis and thorax-segment rotation as viewed from above during different events of the pitching cycle. This figure helps visualize the squaring of the pelvis and thorax to home plate and the relative rotations between these two segments. The numbers provided under each segment reflect the mean (± 1 SD) segment position relative to the global coordinate system (GCS). ASIS, anterior superior iliac spine; L, left; R, right; SJC, shoulder-joint center.

peak elbow varus moment found in our study and the 1999 study by Fleisig et al. (4) is inconsistent with the relatively greater ball and joint velocities found in the 1999 Fleisig et al. study in comparison with our study. This inconsistency can be explained based on modeling differences between the two studies. In 2006, Fleisig et al. (6) reported that his previous peak elbow varus moments were underestimated because of the absence of a hand segment in the biomechanical model. We explored this further by eliminating the hand segment similar to Fleisig et al.'s 2006 paper, and we observed a similar decrease in the elbow moment. By including the hand in our analysis, our lower elbow varus moments are likely more accurate and are consistent with the lower ball velocities.

Ball velocity may also be explained by examining thorax and pelvis motion. Most pitching authorities have stated that the timing of rotation of the pelvis and thorax segments directly impacts pitch velocity, accuracy, and, therefore, loads. We looked at the two and compared their measured parameters. The pelvis was generally more open toward the plate (rotated counterclockwise in a right-handed pitcher) at FC than was the thorax: $-64 \pm 12°$ versus $-92 \pm 11°$, respectively. The internal rotation velocity of the pelvis ($678 \pm 90°\cdot s^{-1}$) and thorax ($938 \pm 109°\cdot s^{-1}$) occurred rapidly, but at slower rates than described in the literature. The slower internal rotation velocity may explain the reduced pitching velocities in the study group in comparison with the literature, because the rotation of the thorax relative to the pelvis has been suggested to have implications with respect to pitch velocity.

The shoulder motion in the current study, when reported using methods similar to the literature (humerus vs trunk), showed only minimal differences between studies. Shoulder abduction at MER and horizontal abduction at MER were very similar between the current study and that of Sabick et al. (12). Shoulder maximal external rotation values in this study were similar to the published literature (current study, $168 \pm 10°$; Sabick et al., $166 \pm 9°$ (12)) and the youth pitchers in the study by Fleisig et al. ($177 \pm 12°$ (4)). Again, MIR velocities were significantly lower in the study group ($3778 \pm 487°\cdot s^{-1}$) in comparison with the youth pitchers in the 1999 paper by Fleisig et al. ($6900 \pm 1050°\cdot s^{-1}$). However, the two groups had similar maximal glenohumeral internal rotation torque (27 ± 12 N·m) compared with adolescents in the 1999 paper by Fleisig et al. (30 ± 7 N·m). As mentioned previously, kinetic values were underestimated in the 1999 study by Fleisig et al.

A limitation of this study was that we measured the adolescent pitchers from a flat surface and not off a mound. At this point, it is not known whether this makes a difference in the kinematic and kinetic measures above. Preliminary work seems to indicate, however, that both ball velocity and joint velocities are increased from the mound. An investigation into this notion is currently underway.

SUMMARY

This report uses computerized motion-analysis technology to evaluate adolescent pitching biomechanics. Only two other studies in the literature, to our knowledge, have evaluated adolescent pitchers in this fashion (4,12). We hope to use this methodology to continue to pursue a further understanding of the pitching biomechanics in this age group. Studies are currently underway to evaluate the effect of different pitch types on these individuals. With a better understanding of pitching biomechanics, we hope to be able to prevent injuries and to better direct our rehabilitative methods, should injuries occur.

The authors would like to acknowledge the entire staff at the Connecticut Children's Medical Center's Center for Motion Analysis as well as Amherst College Baseball Coach Bill Thurston for their time and support.

REFERENCES

1. Axe, M. Recommendations for protecting youth baseball pitchers. *Sports Med. Arthrosc.* 9:147–153, 2001.
2. Escamilla, R., G. Fleisig, S. Barrentine, N. Zheng, and J. Andrews. Kinematic comparisons of throwing different types of baseball pitches. *J. Appl. Biomech.* 14:1–23, 1998.
3. Fleisig, G., J. Andrews, C. Dillman, and R. Escamilla. Kinetics of baseball pitching with implications about injury mechanisms. *Am. J. Sports Med.* 23:233–239, 1995.
4. Fleisig, G., S. Barrantine, N. Zheng, R. Escamilla, and J. Andrews. Kinematic and kinetic comparison of baseball pitching among various levels of development. *J. Biomech.* 32:1371–1375, 1999.
5. Fleisig, G., R. Escamilla, J. Andrews, T. Matsuo, Y. Satterwhite, and S. Barrantine. Kinematic and kinetic comparison between baseball pitching and football passing. *J. Appl. Biomech.* 12:207–224, 1996.
6. Fleisig, G. S., D. S. Kingsley, J. W. Loftice, et al. Kinetic comparison among the fastball, curveball, change-up, and slider in collegiate baseball pitchers. *Am. J. Sports Med.* 34:423–430, 2006.
7. Gugenheim, J. J. Jr., R. F. Stanley, G. W. Woods, and H. S. Tullos. Little league survey: the Houston study. *Am. J. Sports Med.* 4:189–200, 1976.
8. Hang, Y-S. Little league elbow: a clinical and biomechanical study. In: *Biomechanics*, Vol. VIII-A, H. Matsui and K. Kobayashi (Eds.). Champlain, IL: Human Kinetics, pp. 70–85, 1983.
9. Larson, R., K. Singer, R. Bergstrom, and S. Thomas. Little league survey: the Eugene study. *Am. J. Sports Med.* 4:201–209, 1976.
10. Murray, T., T. Cook, S. Werner, T. Schlegel, and R. Hawkins. The effects of extended play on professional baseball pitchers. *Am. J. Sports Med.* 29:137–142, 2001.
11. Rab, G., and K. Petuskey. A method for determination of upper extremity kinematics. *Gait Posture* 15:113–119, 2002.
12. Sabick, M., M. Torry, R. Lawton, and R. Hawkins. Valgus torque in youth baseball pitchers: a biomechanical study. *Shoulder Elbow Surg.* 13:349–355, 2004.
13. Westwell, M., S. Ounpuu, C. Nissen, et al. Comparison of techniques for estimating the shoulder joint center (Glenohumeral joint center). *Gait Posture* 20(Suppl. 1):S21, 2004.

APPENDIX

Detailed Model Description/Illustrations

Marker placement locations:

- -Four on headband
- -C7 and T10 spinous processes
- -Jugular notch
- -Xiphoid process
- -Bilateral ASIS and PSIS prominences
- -Bilateral mid-thighs, knees, and tibias
- -Bilateral heels, lateral malleoli, and second metatarsals
- -Left shoulder acromioclavicular joint
- -Left lateral acromial edge
- -Left lateral elbow epicondyle
- -Bilateral radial and ulnar styloids
- -Bilateral second metacarpals
- -Right coracoid process, anterior acromioclavicular joint, and posterolateral acromial angle
- -Right elbow medial and lateral epicondyle

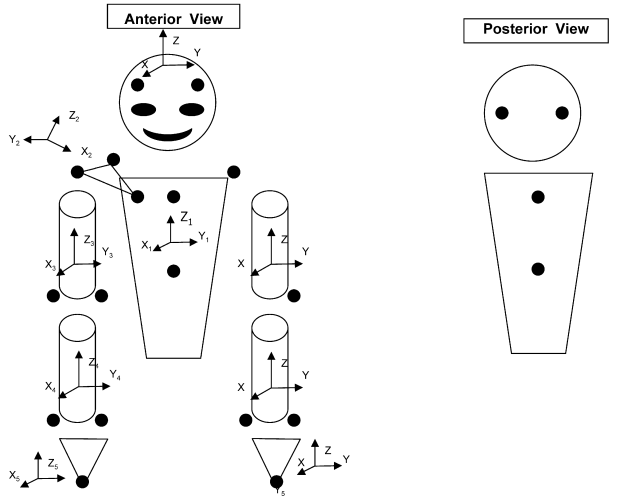

Thorax Segment

Rotational Axis (Z_1) = unit vector defined by UTRX-LTRX
Temp Axis = unit vector defined by BTRX-FTRX
Sagittal Axis (Y_1) = Temp cross Z_1
Coronal Axis (X_1) = Z_1 cross Y_1
UTRX = midpoint between CLAV and C7
LTRX = midpoint between STRN and T10
BTRX = midpoint between C7 and T10
FTRX = midpoint between CLAV and STRN

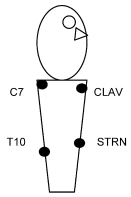

Scapula Segment

Rotational Axis (Z_2) = unit vector defined by RSAC -(RSPC+RSAA)/2
Temp Axis = unit vector defined by RSAA-RSPC
Sagittal Axis (Y_2) = Temp cross Z_2
Coronal Axis (X_2) = Z_2 cross Y_2
Glenohumeral Joint Center (GHJC) calculated using a spherical centering method

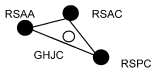

Upper Arm Segment

Rotational Axis (Z_3) = unit vector defined by GHJC - REJC
Temp Axis = unit vector defined by REJC -RWJC
Sagittal Axis (Y_3) = Temp cross Z_3
Coronal Axis (X_3) = Z_3 cross Y_3
Elbow Joint Center (REJC) = midpoint between RELB and REMB

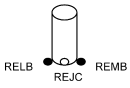

Forearm

Sagittal Axis (Y_4) = Y_3
Temp Axis = unit vector defined by RWJC-REJC
Coronal Axis (X_4) = Temp cross Y_4
Transverse Axis (Z_4) = Y_4 cross X_4
Wrist Joint Center (RWJC) = midpoint between RWRA and RWRB

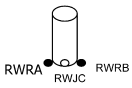

Hand

Rotational Axis (Z_5) = unit vector defined by RWJC – RHND
Temp Axis = unit vector defined by RWRA-RWRB
Coronal Axis (X_5) = Temp cross Z_5
Sagittal Axis (Y_5) = X_5 cross Z_5
RHND = Offset ½ hand thickness along X_5 Axis from RFIN marker